LAWRENCE
LIVERMORE
NATIONAL
LABORATORY

LLNL-TR-826154

Simulating Dopant Diffusion in a Detalied Porous Structure

W. G. Moore, A. P. Lange, K. Sasan, J. Ha, G. D. Kosiba

August 26, 2021

Disclaimer

This work performed under the auspices of the U.S. Department of Energy by Lawrence Livermore National Laboratory under Contract DE-AC52-07NA27344.

Simulating Dopant Diffusion in a Detailed Porous Structure

ABSTRACT

The National Ignition Facility (NIF) at Lawrence Livermore National Laboratory (LLNL) uses high-powered lasers to explore cutting edge fusion technology. Specialized optics, known as fiber lasers, generate and amplify the NIF's high-powered lasers that facilitate fusion experiments. Fiber lasers are glass fibers that are doped with heavy elements to stimulate light emission. The fiber laser doping processing uses a pre-deposited layer of porous silica nanoparticles on the surface of the glass to absorb a dopant rich salt solution. Our project simulated the diffusion of dopants into porous silica with prescribed colloidal stacking geometries using COMSOL Multiphysics. With these simulations we identified the porosity and tortuosity of the porous nanoparticle structures as the primary parameters that will dictate how the dopants will diffusive into the porous surface of the glass. Porosity and Tortuosity are geometric parameters that can easily be input into more detailed simulations to estimate an effective diffusivity within the porous layer. Future work should account for surface reactions to accurately simulate the full-scale diffusion of the solution doping process.

INTRODUCTION

Fiber lasers

Fiber laser manufacturing is a rapidly maturing process as the fiber laser market is valued at 2.3088 billion USD and projected to increase to 4.674 billion USD by 2027. Fiber lasers are lasers made from fiber optics which are long wires of glass that are used to transmit concentrated light. Traditional communication fiber optics are generally doped with one or two index modifying elements such as germanium or fluorine. Fiber lasers on the other hand require additional rare earth ion dopants (i.e., lanthanides) such as ytterbium and other co-dopants to improve the lasing efficient of the luminescent ions. These dopants not only influence the properties of the fiber waveguide, but they also facilitate gain and lasing through light absorption and subsequent stimulated emission. Lasers are made by shining light on an electron to promote it to an excited state, then stimulating the decay of this electron back to the ground state by bombarding the electron with another photon with equal energy. The 4f electrons of lanthanides are shielded from bonding by their 5d and 6s electrons, which leaves the 4f states available and unaltered for the stimulated transitions which emit light. These transitions are also energetically efficient in that not much energy is lost via heat which makes them attractive for high-powered laser generation.[1,2] This makes lanthanides excellent active dopants for a variety of host materials, including silica glasses commonly used in optical fibers.

Fiber lasers have a variety of uses due to their excellent ability to produce high-powered, efficient, and cost-effective laser sources. These laser sources are utilized in metallic 3D printing lasers, the U.S military's high-energy defense lasers, and within the master oscillator of the NIF's 2 Megajoule laser. Fiber lasers begin their life as a thick rod of glass known as a preform, before they are eventually drawn into long, thin fibers ranging from a few hundred micrometers to only tens of microns in diameter. Chemical vapor deposition (CVD) is the typical process for making fiber optic preforms. However, the vapor pressures of the heavy element dopants are far too low near room temperature to be suitable for CVD.[3] The need for these unique heavy element dopants drove the development a four-step liquid-based doping method at LLNL that allows nearly any element to be used as a dopant.

Solution doping and simulation

To begin the liquid-doping process, a layer of porous silica is formed on the interior of an open tube of fused silica glass by dunking the tube in a colloidal solution of silica nanoparticles. These silica nanoparticles are created through a LLNL developed sol-gel process which allows for excellent control of the size of the nanoparticles and the morphology of the porous layer. The tube can then be dip coated into a dopant-salt ethanol solution where the porous silica fills with the dopant saturated liquid. Finally, the tube is heated using a lathe and oxyhydrogen torches and collapsed into the final shape of the preform, with a doped silica core and a pure silica shell. The preform is now ready to be extruded into a doped fiber.[4-6]

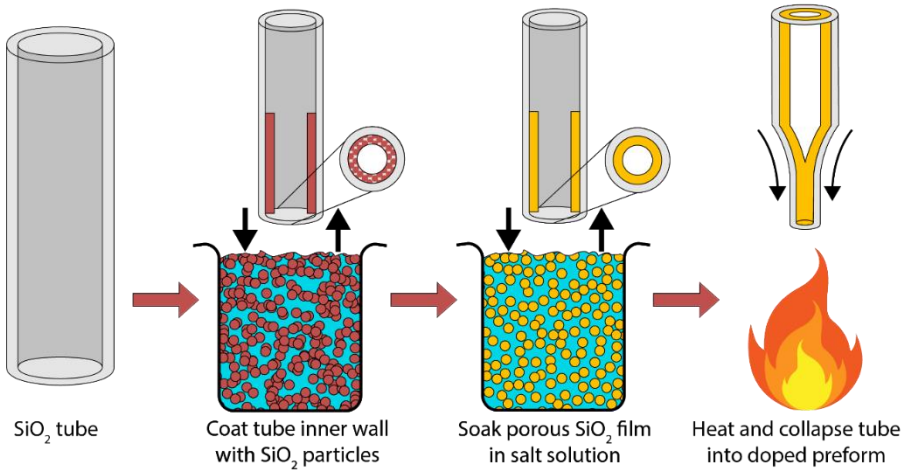

Figure 1. Outline of the LLNL silica fiber laser preform solution doping process.

The solution doping process described in Figure 1 currently faces issues with uncontrolled concentration gradients, specifically a consistent and dramatic decrease in concentration at the core of the preform,[4] such as that seen in Figure 2. Simulations of dopant diffusion within the porous silica glass during the solution doping process are valuable to predict how this concentration gradient arises. However, simulating the geometry of the porous media's nanostructure at the macroscale would take unfeasible amounts of computing power, so instead we derived an effective diffusivity for the motion of the dopants within the porous silica from our simulations.

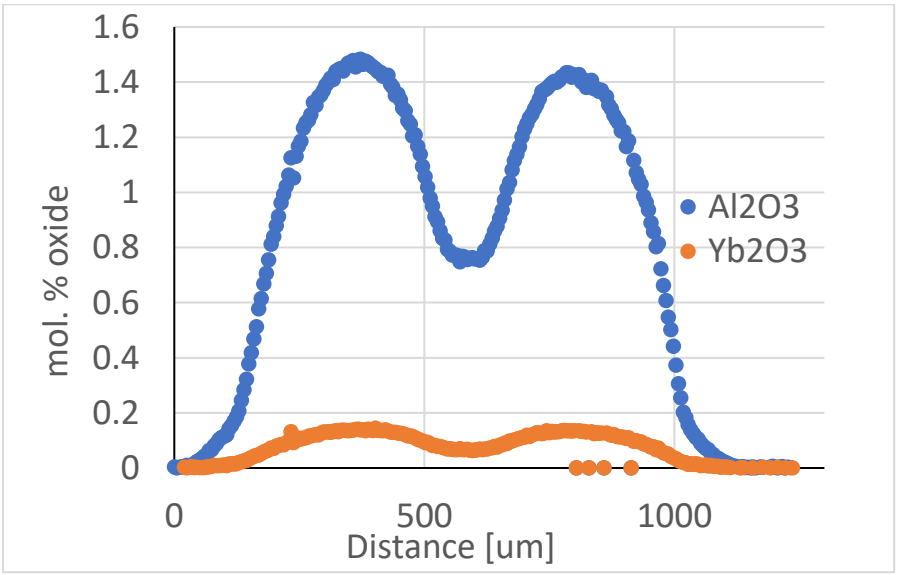

Figure 2. Concentration profiles of Al_2O_3 and Yb_2O_3 dopants across the width of a fiber laser preform core.

We developed COMSOL Multiphysics simulations which use detailed models to represent the porous silica's nanostructure to calculate an effective diffusivity that accounts for the effects of nanoparticles on the diffusion of the dopants. The simulations revealed that two specific geometric parameters: the porosity and tortuosity of the porous silica can be used to define the effective diffusivity of any dopant within the porous structure. Porosity describes the open volume that the dopants can pass through as a fraction of the total volume, while tortuosity is defined as the ratio between the length of a curved path and the distance between the path's endpoints. Tortuosity is difficult to calculate in a non-ideal, 3D system, but our simulations allowed us to calculate the tortuosity of arbitrary silica pore networks while using realistic diffusion parameters. Future work will utilize the calculated porosity and tortuosity within macroscopic models of the dip coating process to realistically simulate how any dopants will diffuse through the porous glass and predict the final composition of the preform cores.

SIMULATIONS

Detailed structures

The effective diffusion simulations were built in COMSOL Multiphysics based on the COMSOL module "Effective Diffusivity in Porous Materials.[7]" Each simulation used a finite element mesh and dilute chemical species transport physics to calculate the time dependent concentration profile of dopants through an artificial porous structure. Four geometric models were produced to vary the porosity and tortuosity between each structure by transforming layers of nanoparticles within each version. From least densely packed to most densely packed the versions were: "low pack," "low pack offset," "medium pack," and "close pack" as shown in Figures 3-6. Arrays of nanoparticle spheres were converted into a working model by subtracting the nanoparticle array from a bounding box, where the remaining volume of the bounding box is the volume through which the dopants can diffuse.

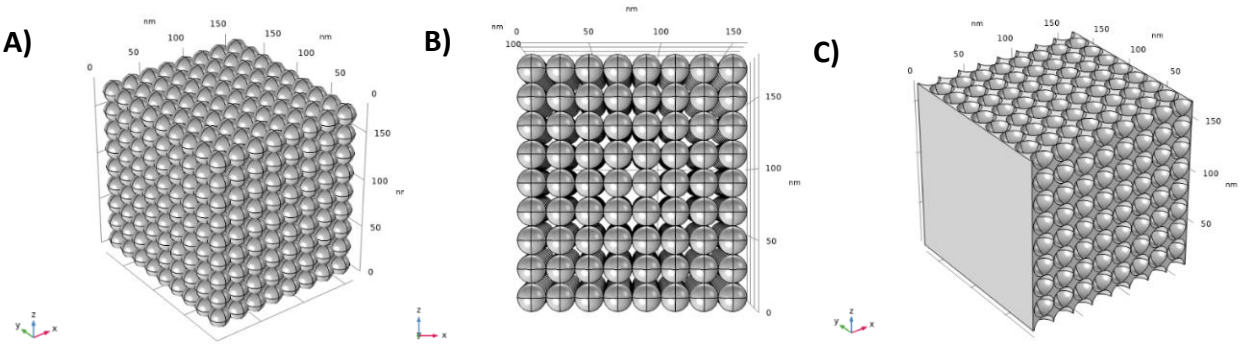

Figure 3. "Low pack" detailed structure. A) and B) show different perspectives of the nanoparticle arrangement prior to the additon of a bounding box. C) shows the nanoparticle structure substracted from the bounding box, forming the flux boundaris of the simulation.

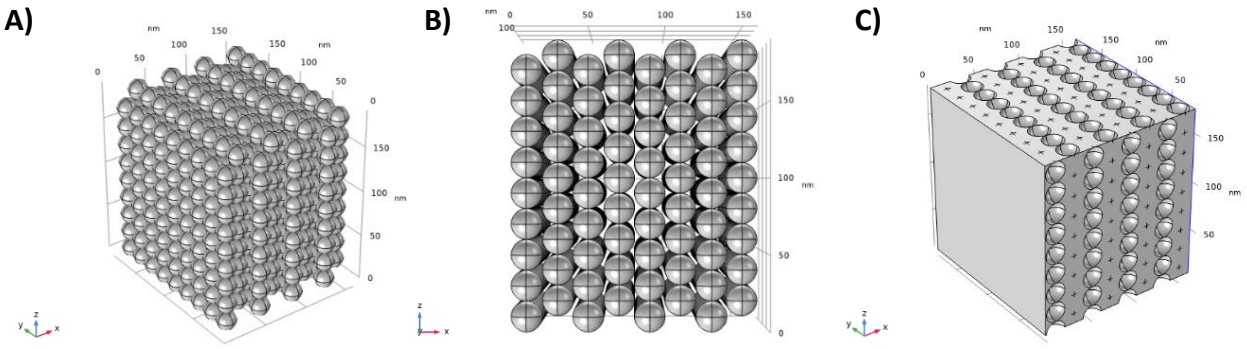

Figure 4. “Low pack offset” detailed structure. A) and B) show different perspectives of the nanoparticle arrangement prior to the additon of a bounding box. C) shows the nanoparticle structure substracted from the bounding box, forming the flux boundaris of the simulation. “Low pack offset” adds an offset to every other particle layer to increase the tortuosity.

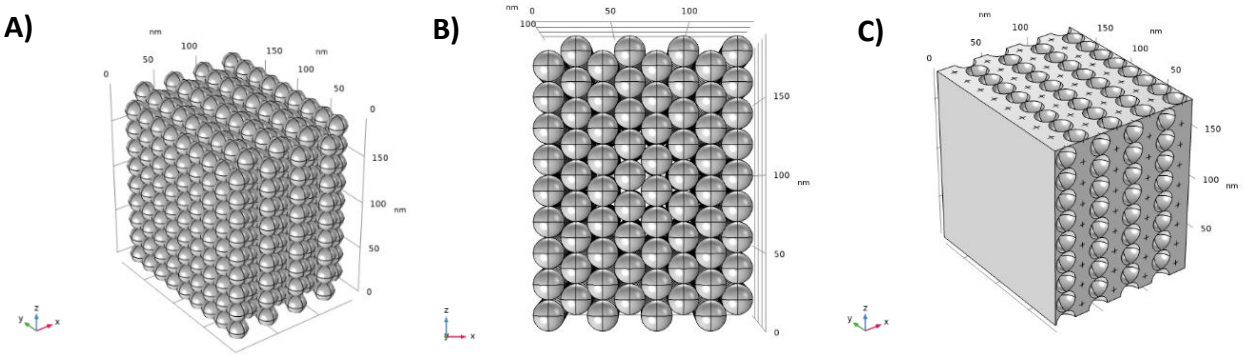

Figure 5. “Medium pack” detailed structure. A) and B) show different perspectives of the nanoparticle arrangement prior to the additon of a bounding box. C) shows the nanoparticle structure substracted from the bounding box, forming the flux boundaris of the simulation. “Medium pack” compresses the layers along the x-axis until each particle layer along the x-axis touches their adjacent layers to decrease the porosity.

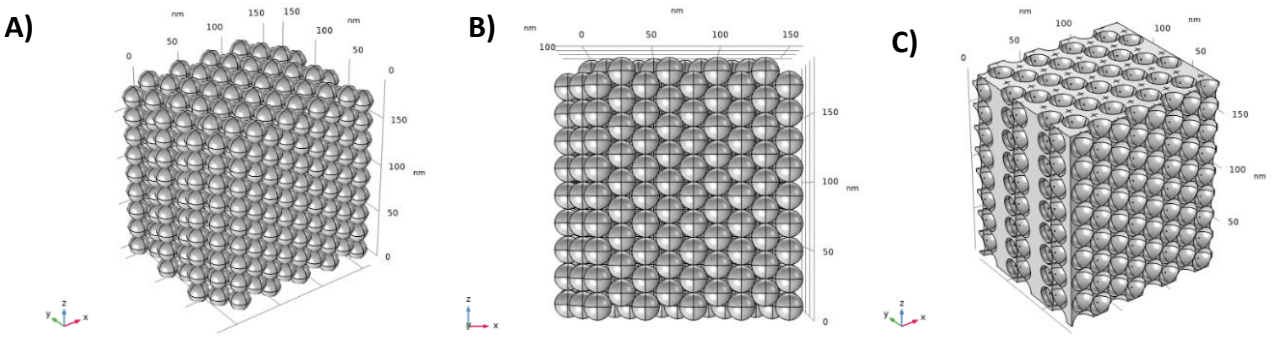

Figure 6. "Close pack" detailed structure. A) and B) show different perspectives of the nanoparticle arrangement prior to the additon of a bounding box. C) shows the nanoparticle structure substracted from the bounding box, forming the flux boundaris of the simulation. "Close pack" is the most tightly packed cell possible, designed to imitate a face centered cubic crystal structure.

The difusion of dopant ions was simulated through each of these models assuming an ethanol solution had instantaneously filled the porous structure. The dopant gradually diffused along the x-axis because the leftmost y-z face (x = 0) of each model is a concentration boundary and the opposing rightmost y-z face is a flux boundary. All other external and internal surfaces of the simulation prohibited diffusion, creating a sort of tunnel filled with impassible nanoparticles. These nanoparticles slow the transport of dopant species through the model, which is represented as an effective diffusion coefficient that is lower than the "free" diffusion coefficient of the dopants in the saturated solution.[7]

Simulation calculations

The diffusion is calculated using Fick's Second Law:

$$\frac{\partial c}{\partial t} + \nabla \cdot (-D\nabla c) = 0 \qquad \textbf{(1)}$$

Where *t* is time, *c* is concentration and *D* is the free diffusivity coefficient. Along the x-axis the leftmost y-z face is assigned as a fixed concentration boundary of 3 mol/m^3, and the rightmost y-z face is assigned as a flux boundary governed by the following relationship:

$$(-D\nabla c) \cdot \boldsymbol{n} = k_m(c - c_1) \qquad \textbf{(2)}$$

Where $\boldsymbol{n}$ is a unit vector perpendicular to the boundary face, c_1 is the concentration beyond the rightmost face (assumed to be 0 mol/m^3) and k_m is the mass transfer coefficient. The mass transfer coefficient is an important controlled parameter that describes the movement of dopant species through the simulation. Through multiple tests, it was concluded that if the mass transfer coefficient wasn't exceedingly small the simulation would return a consistent tortuosity for each specified geometry.

An initial concentration profile of the dopants was assigned such that the concentration was close to zero throughout the entire *x*-length of the simulation on the first time-step:

$$c(t_0) = c_0 \exp(-ax^2) \quad \textbf{(3)}$$

Where c_0 is the initial concentration defined at the leftmost boundary, and a is an arbitrary exponent constant. With these parameters, the simulation has what it needs to operate. The simulation calculates the concentration gradient across the detailed structure. The parameters for each simulation are displayed in Table 1.

Table 1. The basic input parameters of the different effective diffusivity simulations.

Simulation version	Low pack	Low pack offset	Medium pack	Close pack
***D* [m²/s]**	2 x 10^{-9}	2 x 10^{-9}	2 x 10^{-9}	2 x 10^{-9}
c_0 [mol/m³]	3	3	3	3
k_m [m/s]	5	5	5	5
***a* [-]**	1000	1000	1000	1000
L_x [nm]	162	162	143.24	143.24
L_y [nm]	160	170	170	130
L_z [nm]	160	170	170	170

The effective diffusivity was calculated by measuring the average flux exiting the model, $N_{average}$ and the average concertation at the flux boundary, c_{out}.

$$D^{eff} = N_{average} \frac{L_x}{(c_0 - c_{out})} \quad \textbf{(4)}$$

Where L_x is the length of the model along the x-axis and D^{eff} is the effective diffusivity. The average flux is evaluated as average over the surface of the rightmost flux boundary:

$$N_{average} = \frac{1}{L_y L_z} \int_0^{L_z} \int_0^{L_y} k_m (c - c_1) dA \quad \textbf{(5)}$$

Where L_y and L_z are the dimensions of the simulation along the y- and x-axes respectively, and *dA* signifies integration of the surface area of the flux boundary. The concentration at the flux boundary is evaluated by the relationship:

$$c_{out} = \frac{1}{L_y L_z} \int_0^{L_z} \int_0^{L_y} c dA \quad \textbf{(6)}$$

With this information the effective diffusivity can be easily calculated using Equation 4. The effective diffusivity must be calculated for each dopant because each dopant has a different "free" diffusivity. However, there is a simple way to calculate an effective diffusivity through a porous media using the porosity, ε, and the tortuosity, τ:

$$D^{eff} = D \frac{\varepsilon}{\tau} \quad \textbf{(7)}$$

The porosity can easily be calculated using COMSOL by calculating the volume fraction of free space for the dopants to diffuse:

$$\varepsilon = \frac{1}{L_x L_y L_z} \int_0^{L_z} \int_0^{L_y} \int_0^{Lx} 1 \, dV \quad \textbf{(8)}$$

Where *dV* indicates that this surface integral is being performed over the entire geometric volume of the simulation. Rearranging Equation 7 we have a simple way to calculate the tortuosity:

$$\tau = D \frac{\varepsilon}{D^{eff}} \quad \textbf{(10)}$$

This final relationship has several benefits. Using our detailed 3D nano-structure simulation we can find the porosity and tortuosity of the porous media using any "free" diffusivity as a starting point. The only limitation to this rule is that the diffusivity must be high enough to progress across the entire simulation in a realistic timescale or the dopant will not reach the flux boundary. With the porosity and tortuosity, we can calculate the effective diffusivity of any dopant using only the porous structure's geometric properties. COMSOL porous media simulations in fact offer the option to use a tortuosity model to calculate the effective diffusivity of a porous media using this precise relationship.

RESULTS AND DISUCSSION

The simulation results in Table 2 and Figures 7-9 confirmed the expected trends that decreasing the porosity and increasing the tortuosity will decrease the effective diffusivity. Offsetting the nanoparticle layers to block open paths, such as in the "low pack offset" arrangement, causes an appreciable jump in tortuosity leading to a decrease in the effective diffusivity. The "medium pack" arrangement reduces the space between particle layers,

decreasing the porosity but also decreasing the tortuosity, possibly because the dopant path length is decreased. “Close pack” had the lowest porosity because the nanoparticles were as tightly packed as possible, and highest tortuosity because the multiple offset planes impeded dopant diffusion.

Table 2: The average concentration at the flux boundary, average flux exiting the simulation, porosity, tortuosity, and effective diffusivity data collected from the four detailed structure diffusion simulations.

Simulation version	Low pack	Low pack offset	Medium pack	Close pack
c_{out} **[mol/m^3]**	0.00268	0.00257	0.00255	0.00145
$N_{average}$ **[mol/(m^{2}s)]**	0.0134	0.0129	0.0127	0.0073
Porosity [-]	0.490	0.494	0.428	0.279
Tortuosity [-]	1.352	1.420	1.406	1.607
D^{eff} **[m^2/s]**	7.25×10^{-10}	6.96×10^{-10}	6.09×10^{-10}	3.47×10^{-10}

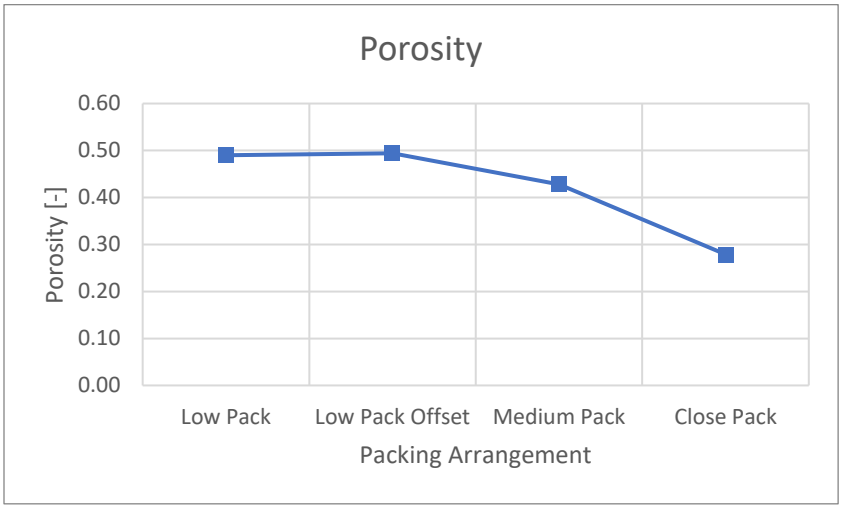

Figure 7. The porosity of the different simulated porous detailed structures.

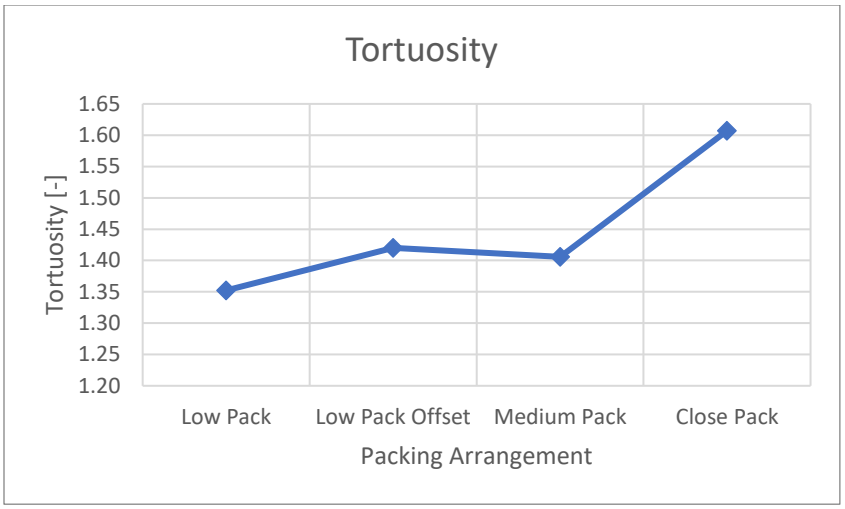

Figure 8. The tortuosity of the different simulated porous detailed structures.

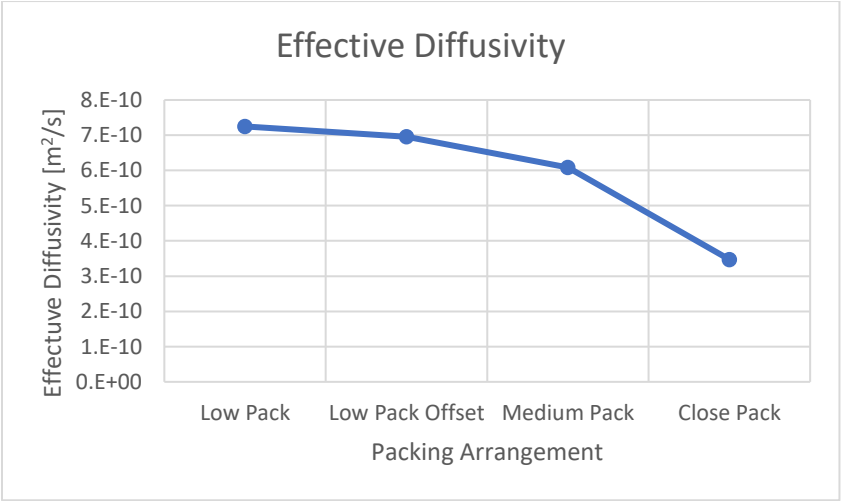

Figure 9. The effective diffusivity of the dopants within the different detailed nanoparticle structures.

These tests were not properly motivated to give us an accurate description of the porous silica, but instead give us helpful insights into how we can adapt our existing model. The porous silica is a disordered array of nanoparticles and is thus likely somewhere between the two effective diffusivity extremes. We can approach a more realistic model through the addition of irregularities such as gaps or stacking faults in the simulated nanoparticle structures.

Simulation bounding

The bounding box of each simulation was built such that all nanoparticles within the simulation were contained with only an extra nanometer along the x-direction on both sides each simulation, excluding the "close packed" model. It was found that changing the model size while scaling all dimensions did not change the porosity or tortuosity of the model, so it was assumed that changing the box containing the nanoparticles would also have no effect. This assumption was untrue for these studies because the bounding box for each different nanoparticle arrangement was not scaled uniformly. A controlled study could have avoided this scaling issue by instead maintaining a constant bounding box size between each simulation and increasing the number of nanoparticles to completely fill the space.

Finite element limitations

The limitations of finite element simulations also introduce some inaccuracy to the simulations. Noticeable differences between the results of high-fidelity fine element mesh simulations and low-fidelity coarse element mesh simulations in Table 3 indicates that the mesh quality strongly impacts the porosity and tortuosity of the model. Figure 10 shows how a course mesh will inaccurately model the nanoparticle spheres compared to a finer mesh. These low polygon spheres less accurately estimate the volume of the nanoparticles, decreasing accuracy of the calculated porosity. Rough sphere edges shrink the cross-sectional area of dopant diffusion paths between the nanoparticles, such as those seen in Figure 10, causing an inaccurate tortuosity measurement. Future work should use the finest mesh size possible to obtain the most accurate results.

Table 3. Comparison of diffusivity data collected using a normal (course) mesh simulation versus a finer mesh simulation in COMSOL.

Simulation mesh version	Close pack normal mesh	Close pack finer mesh
$N_{average}$ **[mol/(m^{2}s)]**	0.00826	0.00727
c_{out} **[mol/m^3]**	0.00165	0.00145
Porosity [-]	0.295	0.279
Tortuosity [-]	1.498	1.607
D^{eff} **[m^2/s]**	3.94×10^{-10}	3.47×10^{-10}

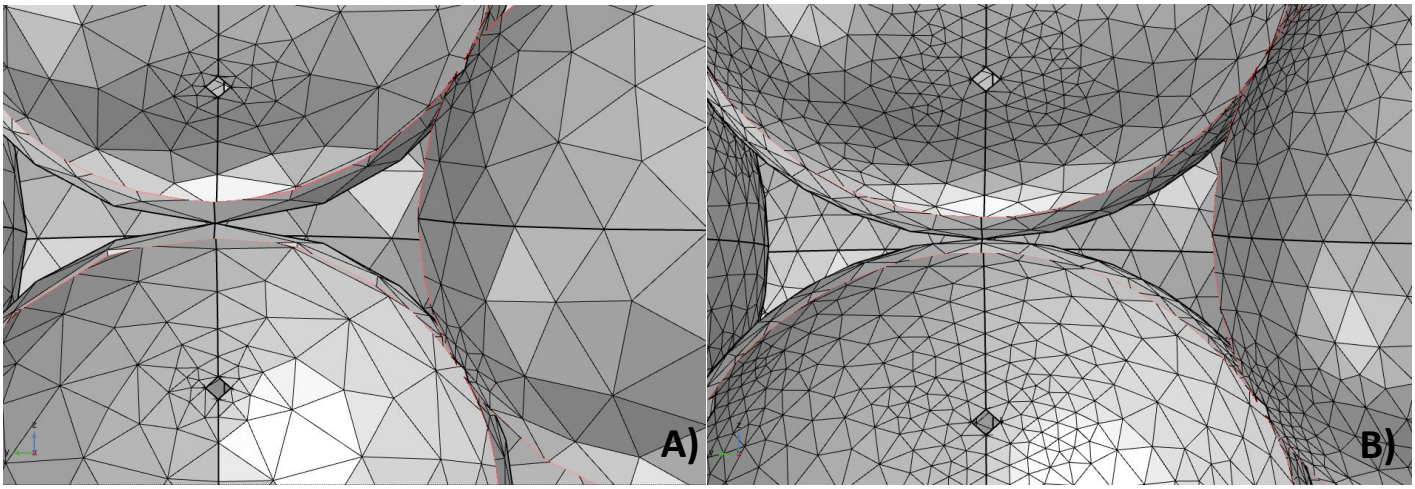

Figure 10. A close-up image of the detailed structure near a triangular diffusion path between nanoparticles for a A) normal (coarse) mesh, and a B) fine fidelity mesh. Notice the rough irregular edges of the coarse mesh compared to the fine mesh. These rough edges impact the effective cross-sectional area available for dopants to diffuse through.

CONCLUSION

The 3D COMSOL detailed structure diffusion simulations are a first step towards preparing a full macroscale simulation. The simulations proved excellent at estimating the porosity and tortuosity of detailed porous structures, particularly for the extrema of possible porous silica nanostructures. Future work will perform parametric studies while controlling the size of the simulation bounding box, using an ultra-fine mesh, introducing irregularities into the nanoparticle arrays, and introducing surface reactions into the simulations. Calculated effective diffusivities will be introduced into macroscale COMSOL porous media simulations to model the concentration profiles of the fiber laser preforms without the need to introduce a detailed structure for the porous material within the large-scale model.

AKNOWLEDGMENTS

Funding for this project was received through the Department of Energy (DOE) Science Undergraduate Laboratory Internships (SULI) program, with additional funding from LDRD 20-ERD-012. Special thanks to Moira Foster for additional advice, support, and expertise as well as Graham Kosiba for overseeing my secondary project. Lawrence Livermore National Laboratory is operated by Lawrence Livermore National Security, LLC, for the U.S. Department of Energy, National Nuclear Security Administration under Contract DE-AC52-07NA27344. LLNL-TR-826154.

WORKS CITED

[1]Weber, Marvin J. "Lanthanide and actinide lasers." 1980. 275-311.

[2]Kirchhof, Johannes, et al. "Dopant interactions in high-power laser fibers." *Optical Components and Materials II*. Vol. 5723. International Society for Optics and Photonics, 2005

[3]Cognolato, L. "Chemical vapour deposition for optical fibre technology." *Le Journal de Physique IV* 5.C5 (1995): C5-975.

[4]Yassin, SZ Muhd, et al. "Fabrication and characterization of solution doped gallium and barium preforms." *2014 IEEE 5th International Conference on Photonics (ICP)*. IEEE, 2014.

[5]Lupi, Jean-François, et al. "Gradual-time solution doping for the fabrication of longitudinally varying optical fibres." *Journal of Lightwave Technology* 36.10 (2018): 1786-1791.

[6]Poole, S. B. "Fabrication of Al/sub 2/O/sub 3/co-doped optical fibres by a solution-doping technique." *1988 Fourteenth European Conference on Optical Communication, ECOC 88 (Conf. Publ. No. 292)*. IET, 1988.

[7]COMSOL, “Effective Diffusivity in Porous Materials,” Module.